



HAL
open science

A few properties in symbolic form about the transverse argumental vibration of a beam excited axially by an harmonic motion transmitted through permanent or intermittent elastic contact.

Daniel Cintra, Gwendal Cumunel, Pierre Argoul

► **To cite this version:**

Daniel Cintra, Gwendal Cumunel, Pierre Argoul. A few properties in symbolic form about the transverse argumental vibration of a beam excited axially by an harmonic motion transmitted through permanent or intermittent elastic contact.. 2017. hal-01581374

HAL Id: hal-01581374

<https://hal.science/hal-01581374>

Preprint submitted on 4 Sep 2017

HAL is a multi-disciplinary open access archive for the deposit and dissemination of scientific research documents, whether they are published or not. The documents may come from teaching and research institutions in France or abroad, or from public or private research centers.

L'archive ouverte pluridisciplinaire **HAL**, est destinée au dépôt et à la diffusion de documents scientifiques de niveau recherche, publiés ou non, émanant des établissements d'enseignement et de recherche français ou étrangers, des laboratoires publics ou privés.



Distributed under a Creative Commons Attribution - NoDerivatives 4.0 International License

Transverse argumental vibration of a beam
excited axially by an harmonic motion
transmitted through permanent or intermittent
elastic contact: a few properties in symbolic form

Daniel Cintra (corresponding author), Gwendal Cumunel
Université Paris-Est,
Laboratoire Navier (UMR 8205), CNRS, ENPC, IFSTTAR,
6 et 8, avenue Blaise Pascal,
Cité Descartes, Champs-sur-Marne,
F-77455 Marne La Vallée Cedex 2, France.
email: daniel.cintra@enpc.fr, gwendal.cumunel@enpc.fr

and

Pierre Argoul
IFSTTAR, Laboratoire MAST-SDOA,
F-77455 Marne La Vallée, Cedex 2, France
email: pierre.argoul@ifsttar.fr

Abstract

The transverse argumental vibration of a beam excited axially by an harmonic motion transmitted through intermittent or permanent elastic contact is studied. Previous results have shown, using a smooth model and the averaging method, that a vibration in the fundamental transverse mode of the beam can occur when the frequency of the excitation is an even multiple (greater than 2) of the frequency of the fundamental transverse mode. A few properties of the smooth model are brought out in symbolic form, namely the conditions of occurrence of the stationary regime, formulas pertaining to the excitation threshold, and the precision of the assessment of said thresholds. An all-case upper bound of the relative error about the value of the excitation threshold is given.

Keywords— non-linear; argumental oscillator; beam; axial excitation; transverse; spatial modulation; Van der Pol representation.

Contents

1	Introduction.	4
2	System configuration.	4
3	Stationary condition.	4
	Notations:	4
	Results of the averaging method.	6
	Basic equation of the amplitude in stationary condition.	7
	β -curve, G -curve and stationary-solutions curve.	7
	Excitation threshold.	7
	Stationary-solutions curve.	8
	Restriction on ρ_{00}	9
3.1	Intersection of the β -curve and the G -curve.	9
	Case $1 < \rho_{00}$	11
	Case $\rho_{00} < 1$	13
	A simple criterion to compare a_T and a_0	14
3.2	Graphical representation of the argumental phenomenon's possibility of existence.	14
3.3	Validity of the localization of the minimum of the stationary-solutions curve as the intersection of the β -curve and the G -curve.	19
	Parameterized β -curves.	19
	Parameterized G -curves.	20
	Approached stationary-solutions curve about (A_0, a_0)	21
	Upper bound of the relative error.	22
	The grey zone.	22
	The orange zone.	22
	Points in the orange zone where the relative error vanishes.	24
	A point in the orange zone which is not included in the grey zone.	25
	A point included in both the orange zone and the grey zone.	25
	Contact condition between the borders of the grey zone and the orange zone.	25
	Intersection of the borders of the grey zone and the orange zone.	25
	Conclusion about the relative error.	26
3.4	Approximate symbolic solution for the intersection above the critical line.	26
4	Conclusion.	29
5	Appendix A: tangency condition between the upper β-curve and the upper G-curve.	30
	Equation of the intersection between $a_{A1}(a)$ and $a_{A2}(a)$	30

Function $y_1(z) = E \left(1 - \frac{1}{z} + \frac{1}{z\sqrt{2z+1}} \right)$	30
Function $y_2(z) = \frac{1}{z} \left(\frac{\sqrt{1+z}-1}{\sqrt{z}} \right)^n$	30
Tangency of functions $y_1(z)$ and $y_2(z)$	31
Basis for a numerical study	32

6 Appendix B: position of the G -curve versus the critical line. 35

Notation	35
Definition domain.	35
Limit at 0 and at $+\infty$	35
Direction of variation.	36
Intersection with the critical line.	36
Allowed values for ρ and ρ_{00}	36
Conclusion.	37

1 Introduction.

The so-called argumental oscillator has a stable motion consisting of a periodic motion at a frequency next to its natural frequency when submitted to an external force whose frequency is close to a multiple of said natural frequency. One condition for the phenomenon to arise is that the external force be dependent on the space coordinate of the oscillator. An oscillator exhibiting such characteristics has been described [1] in 1938. The word "argumental" was forged in [10]. Further developments were carried out [8,9], particularly the multiple resonance and the quantum effect. Argumental oscillations have also been observed and described in [7,11]. They have also been studied in [2–4].

In this paper, the transverse argumental vibration of a beam excited axially by an harmonic motion transmitted through intermittent or permanent elastic contact is studied. Previous results [5] have shown that this system obeys an argumental equation, and, using a discontinuous natural model with numerical calculus, as well as a smooth continuous model with the averaging method, that a vibration in the fundamental transverse mode of the beam can occur when the frequency of the excitation is an even multiple (greater than 2) of the frequency of the fundamental transverse mode. Experimental results pertaining to this configuration are given in [6].

2 System configuration.

The schematic system configuration is as shown in Fig. 1. A beam is represented, with its left end S and right end M, in an clamped-(clamped-guided) configuration. Point M is intermittently pushed to the left by a plate C, which is linked to a point A via a spring. \vec{F} is the force intermittently applied by plate C to the beam's right end in M. F is negative when the beam is in compression. Point A is in harmonic motion horizontally in the figure, in such a manner that the contact between plate C and point M be intermittent when the beam and point A are vibrating. When the beam is in resting (i.e. rectilinear) position and point A is in center position, the force applied to point M is denoted by F_0 .

3 Stationary condition.

The argumental transverse vibration of an axially-excited beam has been modeled and studied via the averaging method [5], with the help of a smooth model, to derive the results summarized below.

Notations:

- ν is the angular frequency of the excitation source at point A,
- F_0 is the force F when the beam is at rest and point A is at rest in central position,

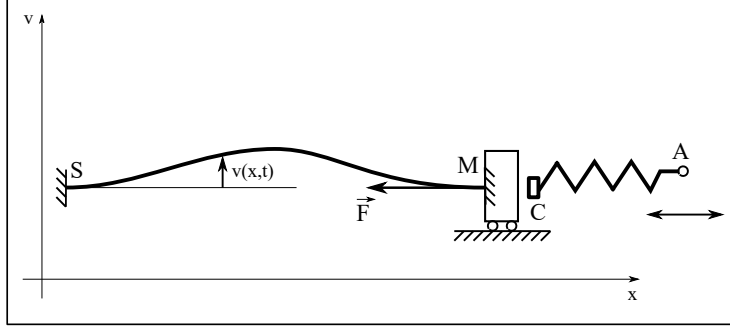


Figure 1: system configuration. x is the horizontal abscissa, v is the transverse displacement, t is the time, and \vec{F} is the force applied by plate C to the beam at point M.

- F_B is the beam's critical buckling force,
- ω_0 is the beam's natural angular frequency when point A is at rest in its central position, with $\omega_0^2 = a_1 \left(\frac{\pi}{L}\right)^2 \frac{F_B + F_0}{\mu S}$, where $a_1 = 1$ in the hinged-(hinged-guided) case, and $a_1 = 4/3$ in the clamped-(clamped-clamped) case, μ =mass per volume unit of the beam, S = section of the beam,
- ω_{00} is the value of ω_0 when $F_0 = 0$,
- n is an even integer roughly equal to $\frac{\nu}{\omega_0}$,
- ρ is a parameter, generally close to 1, chosen so as to have $\frac{\nu}{\rho\omega_0} = n$,
- k is the spring's stiffness,
- L is the beam's length,
- aL is the amplitude of the beam's motion (a is adimensioned),
- $a_S L$ is the amplitude of the beam's stationary-motion (a_S is adimensioned),
- $a_A L$ is the amplitude of the excitation at point A (a_A is adimensioned),
- ρ_{00} is defined as $\rho \sqrt{\frac{F_B}{F_B + F_0}}$,
- a_{Acrit} is a parameter defined as $a_{Acrit} = -\frac{F_0}{kL} = \frac{|F_0|}{kL}$,
- B and C are constants defined as $B = -\frac{\pi^2}{2} \frac{kL}{F_0} = \frac{\pi^2}{2 a_{Acrit}}$ and $C = 2 B$,

- The “Model validity upper limit” is the value which a_A must not exceed for the buckling force never to be exceeded [5], i.e. $\frac{F_B + F_0}{kL}$,

- A is a function of a_A defined as

- If $a_A < a_{Acrit}$:

$$A(a_A) = \frac{kLa_A}{F_B + F_0} \quad (1)$$

which, in this case, is actually independent of a_A .

- If $a_A \geq a_{Acrit}$:

$$A(a_A) = -\frac{F_0 - a_A kL}{2F_B + F_0 - a_A kL} \quad (2)$$

- S_n and D_n are two functions of a defined as

$$S_n(a) = \frac{4}{a^{n+1}} \frac{(\sqrt{1 + Ba^2} - 1)^n}{B^{\frac{n}{2}+1}} \quad (3)$$

$$D_n(a) = \frac{S_n(a)}{\sqrt{1 + Ba^2}} \quad (4)$$

Moreover:

$$\frac{1}{S_n} \frac{\partial S_n}{\partial a} = \frac{1}{a} \left(\frac{n}{\sqrt{1 + Ba^2}} - 1 \right) \quad (5)$$

- G is a function of a and a_A defined as

- If $a_A < a_{Acrit}$:

$$G(a, a_A) = -\frac{1}{2} \frac{F_0}{F_B + F_0} a \left(1 - \frac{2}{Ca^2} + \frac{1}{Ca^2} \frac{2}{\sqrt{1 + Ca^2}} \right) \quad (6)$$

which, in this case, is actually independent of a_A .

- If $a_A \geq a_{Acrit}$:

$$G(a, a_A) = -\frac{1}{2} \frac{F_0 - a_A kL}{2F_B + F_0 - a_A kL} a \left(1 - \frac{2}{Ca^2} + \frac{1}{Ca^2} \frac{2}{\sqrt{1 + Ca^2}} \right) \quad (7)$$

Results of the averaging method. The averaging method consists here in searching a solution close to a slowly-varying sinusoid, carrying out the following classic change of variables

$$\begin{cases} z(\tau) &= a(\tau) \sin(\rho\tau + \varphi(\tau)) \\ \dot{z}(\tau) &= a(\tau)\rho \cos(\rho\tau + \varphi(\tau)) \end{cases}$$

where the dot notation denotes the differentiation w.r.t. reduced time τ .

With the system configuration studied in this paper, the averaging method

yields, among others, the following result: knowing that $n = \frac{\nu}{\rho\omega_0}$ is an even integer, then the system obeys the following system of equations:

$$\begin{cases} \dot{a}(\tau) &= \frac{A(a_A)}{4\rho} S_n(a) \sin(n\varphi(\tau)) - \beta a \\ \dot{\varphi}(\tau) &= \frac{G(a, a_A)}{a} + \frac{A(a_A)}{4a} D_n(a) \cos(n\varphi(\tau)) - \frac{\rho^2 - 1}{2} \end{cases} \quad (8)$$

where $\varphi(\tau)$ is the motion's phase shift w.r.t. the excitation force. Under certain initial conditions, and when some relations between the parameters are satisfied, there is a stationary solution to system (8), namely $z(\tau) = a_S \sin(\rho\tau + \varphi_S)$, where a_S and φ_S are constants, which satisfies the system (8) in which \dot{a} and $\dot{\varphi}$ are set to 0. From this system, a number of symbolic relations will be derived in this paper, which give clues about the stationary condition.

Basic equation of the amplitude in stationary condition. Eliminating φ_S by writing that $\sin^2(n\varphi_S) + \cos^2(n\varphi_S) = 1$, obtain from Eqs. (8):

$$(4\rho\beta)^2 + 4 \frac{S_n^2(a_S)}{D_n^2(a_S)} (2G_1(a_S) - (\rho^2 - 1))^2 = \frac{A^2(a_A) S_n^2(a_S)}{a_S^2} \quad (9)$$

β -curve, G -curve and stationary-solutions curve. To help visualizing some results hereinafter, define a F_β function of variable a_S by

$$F_\beta(a_S) = (4\rho\beta)^2 - \left(\frac{A(a_A) S_n(a_S)}{a_S} \right)^2,$$

and define the “ β -curve” as the curve representing the solution to equation $F_\beta(a_S) = 0$. Also, define a F_G function of variable a_S by

$$F_G(a_S) = 2G_1(a_S) - (\rho^2 - 1),$$

and define the “ G -curve” as the curve representing the solution of

$$F_G(a_S) = 0. \quad (10)$$

Finally, define the “stationary-solutions curve” as the curve representing the solution to Eq. (9). Then, Eq. (9) can be written:

$$F_\beta(a_S) + 4 \frac{S_n^2(a_S)}{D_n^2(a_S)} F_G^2(a_S) = 0 \quad (11)$$

Excitation threshold. It is of interest to be able to assess the minimum value a_{Amin} of a_A versus a_S along a stationary-solutions curve, because this value of a_A is the excitation threshold allowing the argumental phenomenon to arise with given parameters $n, \beta, F_B, F_0, L, k, f_{00}$ and ρ_{00} . The numerical plots show that

the minimum of a_A seems to be close to an intersection point of the β -curve and the G -curve. Therefore, it is natural to carry out a local study around said intersection point to confirm this impression. Said local study will be given hereinafter in Section 3.3. Using a classical approach, by differentiation of Eq. (9), leads to an intricate calculus, with no significant simplification in sight. However, this differentiation leads to guess that $F_\beta(a) \approx 0$ and $F_G(a) \approx 0$ at the minimum of the stationary-solutions curve.

Stationary-solutions curve. Fig. 2 shows the implicit stationary-solutions curve, obtained numerically, giving a_A against a_S for the values of parameters given in the figure’s legend. The solid-line curve represents the stationary-solutions curve of Eq. (9), with a minimum at point A_{min} , which is close to the calculated point of intersection of the β -curve and the G -curve. The solution

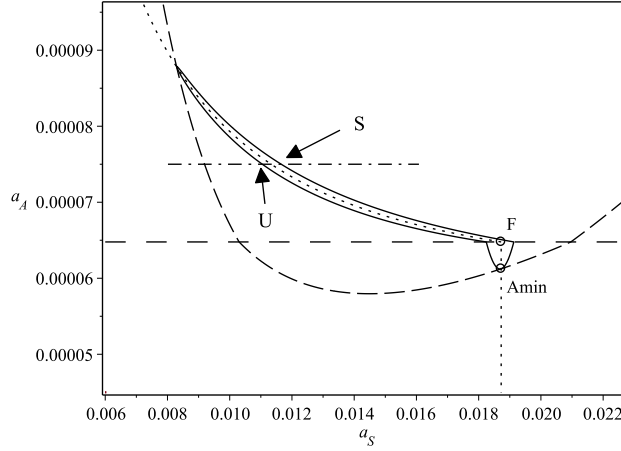


Figure 2: Stationary condition in the case $\rho_{00} < 1$ for the averaged system with the smooth model of the external force. a_S is the stationary-motion’s amplitude, a_A is the excitation’s amplitude. The dotted line is the G curve. The solid line is the locus of the stationary solutions to the averaged smooth model. The dashed line is the β -curve. S and U respectively represent the stable and the unstable stationary conditions located at the intersection of the stationary-solutions curve and the dash-dotted line representing the excitation level. The space-dashed horizontal line is the “critical line”. Below said line, A_{min} is the minimum of the stationary-solutions curve. Parameter values are: $n = 6$, $\beta = 2.4 \cdot 10^{-3}$, $F_B = 51N$, $F_0 = -8N$, $L = 0.95m$, $k = 130 \text{ kN/m}$, $f_{00} = 6.615Hz$, $f_{shaker} = 39.500711Hz$, $\rho_{00} = 0.9952308$, $\lambda = 0.1569$. Model validity upper limit= $4.48 \cdot 10^{-4}$.

to System (8) can be seen as composed of two parts, depending on the position with respect to the horizontal line $a_A = a_{Acrit} = |F_0|/(kL)$, herein called the “critical line”:

- An upper part (above said line) composed of two arcs, in contact at their higher extremities at one point, and at their lower extremities at said line.
- A lower part, constituted by a V-shaped curve, presenting a minimum at point A_{min} .

The upper and lower parts are connected at the critical line. The right (resp. left) arc and the right (resp. left) part of the V-shaped curve represent the stable (resp. unstable) stationary solutions. For a given value of the excitation, i.e. a given amplitude a_A , there are two possible values for a_S , represented by points S and U . Point S is the stable stationary condition, while point U is the unstable one. The V-shaped curve represents cases where there is permanent contact between the beam under test (BUT) and the excitation source when the BUT is in rectilinear position. In these cases, the contact may or may not remain permanent when the BUT enters a transversal vibration, depending on the spring's stiffness and the amplitudes of transversal vibration of the BUT and of the excitation source.

Restriction on ρ_{00} . Appendix B in Section 6 shows that only the values of ρ_{00}^2 comprised between $1 - \lambda$ and 1 are valid to be in the case where a V-shaped part exists. The calculus below are focused on the case $\rho_{00} < 1$, because when $\rho_{00} > 1$, there is no V-shaped part of the stationary-solutions curve, which is entirely above the critical line at ordinate a_{Acrit} ; in this case, it is sufficient to take, as a minimum excitation threshold, the asymptotic limit of the G -curve when $a_S \rightarrow +\infty$, given in Appendix A in Section 5 as $2(1 - 1/\rho_{00}^2)(F_B + F_0) - F_0$. Fig. 3 shows the layout of the curves when $\rho_{00} > 1$: as the G -curve (dotted line) never intersects the critical line, the intersection between the G -curve and the β -curve never exists under the critical line, and therefore, the V-shaped part of the stationary-solutions curve never shows up.

3.1 Intersection of the β -curve and the G -curve.

In this section, the intersection conditions of the β -curve and the G -curve will be studied. The primary focus is not to give a general solution for any configuration of the β -curve and the G -curve, but to bring out some limit configurations, i.e. tangency conditions between said curves, corresponding to limit conditions of possibility for the argumental phenomenon to arise. Those curves each have two different versions: the upper version and the lower version. The upper (resp. lower) versions are applicable when the point representing the stationary condition in the (a_S, a_A) -plane is located above (resp. below) the critical line $a_A = |F_0|/(kL)$. But for the study in this section, the upper versions will be prolonged in the region located below the critical line, for reasoning purposes only. Call “forking point” F the point of intersection of the G -curve with the critical line. The top of lower G -curve is said forking point. Define a_0 as the abscissa of said point.

Compare the upper versions, including their prolonged parts, and study the

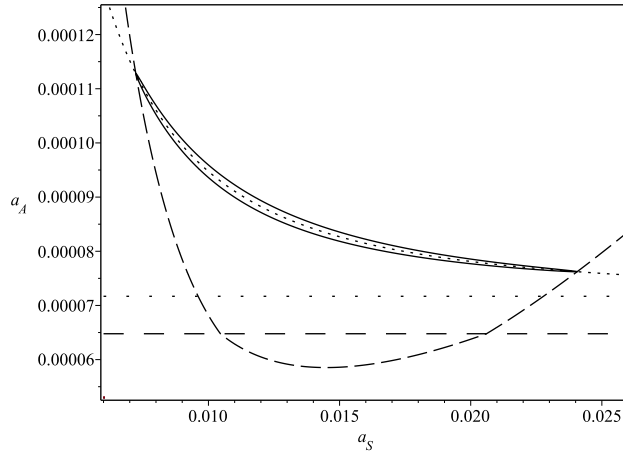


Figure 3: Stationary condition in the case $\rho_{00} > 1$ for the averaged system with the smooth model of the external force. The space-dotted line is the asymptote of the G -curve when $a_S \rightarrow +\infty$. Other graphical-element descriptions and parameter values are the same as for Fig. 2, except $f_{shaker} = 39.88845Hz$ and $\rho_{00} = 1.005$.

tangency condition between the upper β -curve and the upper G -curve. When the tangency point is above the critical line, a slight contraction of the β -curve upon the vertical direction (due to a lower value of β) starting from the tangency condition, will produce two points of intersection between said curve and the G -curve. Those points will both be above the critical line. The rightmost point is close to the minimum of the crescent-shaped stationary-solutions curve representing the stationary conditions of the averaged system. Now if the tangency point is below the critical line, a slight contraction on the β -curve will also produce two points of intersection, but those points will be at the right of the vertical segment constituting the lower G -curve, and therefore, they will not be on the lower G -curve. It will be necessary to apply a stronger contraction on the upper β -curve, until it intersects the G -curve at its forking point. Then, substituting the lower β -curve for the upper β -curve, a slight contraction on the lower β -curve will produce two points of intersection with the G -curve, one located on the upper G -curve, the other on the lower G -curve. This latter point is the point of interest. It is close to the minimum of the V-shaped part of the stationary-solutions curve representing the stationary conditions of the averaged system. Said substitution is legitimate, because the prolonged upper β -curve and the lower β -curve intersect each other at the critical line, so that continuity is preserved.

So, in the upper part of the (a_S, a_A) -plane (above the critical line), the tangency of the β -curve and the G -curve is the limit condition for the intersection of said curves to exist, and then for the existence of solutions to the averaged system.

In the lower part of the plane, the limit condition is when the lower β -curve goes through the G -curve's forking point. However, an approaching method is given at the end of this section, to assess the intersection of the β -curve and the G -curve.

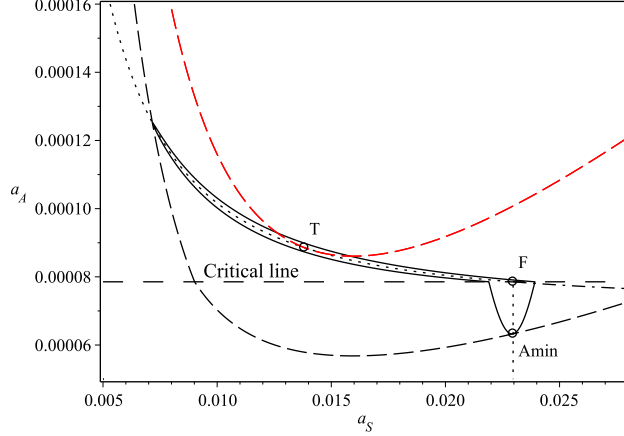


Figure 4: Tangent upper β -curve, case $\rho_{00} < 1$ and $a_T < a_0$. Parameters and description are the same as for Fig. 2, except $F_0 = -9.7N$. The solid curve is the set of stationary solutions curve to the averaged system. F is the forking point. The G -curve is the dotted curve. The upper dashed beta curve is tangent at T to the G -curve. The β -curve giving the minimum value of a_A is the lower dashed curve. The horizontal space-dashed line is the critical line. Model validity upper limit= $3.34 \cdot 10^{-4}$.

Case 1 $< \rho_{00}$. Denote $a_{A1}(a)$ for the upper G-function, which writes:

$$a_{A1}(a) = \frac{F_0}{kL} + 2 \frac{F_B}{kL} \frac{(\rho^2 - 1)Ca^2}{\rho^2 Ca^2 - 2 + \frac{2}{\sqrt{Ca^2 + 1}}}$$

and denote $a_{A2}(a)$ for the upper β -function, which writes:

$$a_{A2}(a) = \frac{F_0}{kL} + 2 \frac{F_B}{kL} \frac{1}{1 + \frac{1}{\rho\beta} \frac{1}{Ba^2} \left(\frac{\sqrt{1+Ba^2}-1}{\sqrt{Ba^2}} \right)^n}$$

Using Eq. (50) of Appendix A, the tangency condition between the upper β -curve and the upper G -curve is:

$$\frac{\rho\beta}{\rho^2 - 1} \approx \frac{4n^2}{(n^2 - 4)^2} \left(\frac{n-2}{n+2} \right)^{n/2} \quad (12)$$

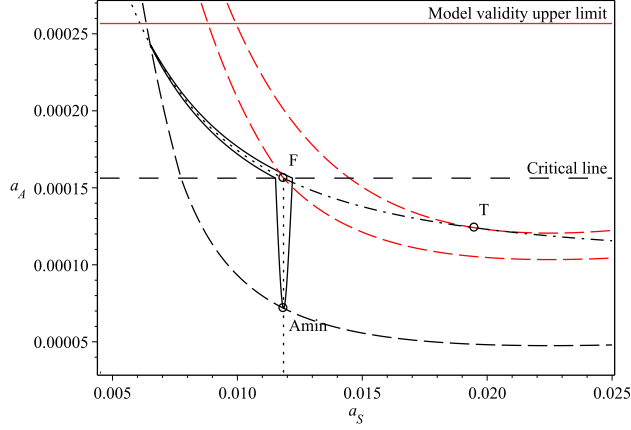


Figure 5: Tangent upper β -curve, case $\rho_{00} < 1$ and $a_0 < a_T$. Parameters and description are the same as for Fig. 2, except $F_0 = -19.3N$, $f_{shaker} = 37.7055 Hz$, $\rho_{00} = 0.95$. The solid curve is the set of stationary solutions to the averaged system. F is the forking point. The prolonged G -curve in the domain located below the critical line is the dot-dashed curve. The upper dashed beta curve is tangent to the prolonged G -curve at point T. The dashed β -curve going through point F is the limit β -curve having an intersection with the G -curve. The β -curve giving the minimum value of a_A along the stationary-solutions curve is the lower dashed curve. The horizontal space-dashed line is the critical line. The Model validity upper limit is visible on the graph.

Substituting $\rho_{00}^2 \frac{F_B}{F_B + F_0}$ for ρ^2 yields:

$$\frac{\rho_{00} \sqrt{1-\lambda}}{\rho_{00}^2 - 1 + \lambda} \beta < \frac{4n^2}{(n^2 - 4)^2} \left(\frac{n-2}{n+2} \right)^{n/2} \quad (13)$$

with $\lambda = \frac{|F_0|}{F_B} = \frac{-F_0}{F_B}$.

To see how this condition translates in the (λ, ρ_{00}) -plane, carry out some calculus, putting $x = 1 - \lambda$, $y = \rho_{00}^2$, $F = \frac{4n^2}{(n^2 - 4)^2} \left(\frac{n-2}{n+2} \right)^{n/2}$, and $c = 1 + \frac{1}{2F^2}$, to obtain the inequality

$$(y - cx)^2 - (c^2 - 1)x^2 > 0 \quad (14)$$

which in turn yields

$$\begin{cases} y > (c + \sqrt{c^2 - 1})x \\ or \\ y < (c - \sqrt{c^2 - 1})x \end{cases} \quad (15)$$

Getting back to the original parameters λ and ρ_{00} , obtain:

$$\begin{cases} \lambda > 1 - \frac{\rho_{00}^2}{c + \sqrt{c^2 - 1}} \\ or \\ \lambda < 1 - \frac{\rho_{00}^2}{c - \sqrt{c^2 - 1}} \end{cases} \quad (16)$$

Because $c > 1$ by definition, the second condition cannot be satisfied if $\rho_{00} > 1$. It remains the first condition, meaning that the representative point in the (λ, ρ_{00}) -plane must be above an horizontal-axis parabola. The condition is expressed by the inequation

$$\lambda > 1 - \frac{\rho_{00}^2}{c + \sqrt{c^2 - 1}} \quad (17)$$

Said point must also be under the parabola of equation $\lambda = 1 - \frac{\rho_{00}^2}{2}$ because of condition (60) given in Appendix B.

Case $\rho_{00} < 1$. Denote a_T for the abscissa of the tangency point between the limit upper β -curve and the upper G -curve. Here two cases must be distinguished, depending on the relative abscissae a_T and a_0 of the tangency point and the G -curve's forking point. The expression of a_0^2 is given in Eq. (21) and the expression for a_T^2 in Eq. (53). A simple criterion to compare a_T and a_0 is given hereinafter.

- If $a_T < a_0$, the intersection points of the limit β -curve and the G -curve are both above the critical line, and consequently are on the upper parts of said curves. Therefore, the limit intersection condition of said curves is the same as for the case $\rho_{00} > 1$.
- If $a_0 < a_T$, it has been showed above that the limit intersection condition is constituted by the lower β -curve going through the G -curve's forking point. The lower β -function is

$$a_A(a) = \rho_{00}\beta \frac{\sqrt{F_B(F_B + F_0)}}{kL} \frac{1}{\frac{1}{Ba^2} \left(\frac{\sqrt{1+Ba^2}-1}{\sqrt{Ba^2}} \right)^n} \quad (18)$$

The condition for the lower β -curve and the lower G -curve to intersect is

$$a_A(a_0) < a_{Acrit} \quad (19)$$

where a_0 is the forking point's abscissa. Eq. (59) gives the expression of a_0 .

Then substitute a_0 for a in Equ (19) using Eq. (18) to obtain the condition of intersection below the critical line:

$$\beta < \frac{\lambda}{\rho_{00}\sqrt{1-\lambda}} \frac{1}{Ba_0^2} \left(\frac{\sqrt{1+Ba_0^2}-1}{\sqrt{Ba_0^2}} \right)^n \quad (20)$$

Then transform the expression Ba_0^2 using Eqs (59) and the definition of constant B to obtain

$$Ba_0^2 = \frac{\lambda}{1 - \rho_{00}^2} - \frac{1}{4} - \frac{1}{4} \sqrt{1 + 8 \frac{\lambda}{1 - \rho_{00}^2}} \quad (21)$$

and finally substitute this expression of Ba_0^2 into (20) to obtain a condition based only on parameters λ , ρ_{00} , β and n , valid when $\rho_{00} < 1$ and $a_0 < a_T$.

Finally, conditions (17) and (20) allow to plot in the (λ, ρ_{00}) -plane, for given values of β and n , the regions where the argumental phenomenon can arise.

A simple criterion to compare a_T and a_0 . Here it is assumed that $\rho_{00} < 1$. To form the criterion, firstly consider the case $a_T < a_0$. Using the expressions of a_0^2 from Eq. (21) and a_T^2 from Eq. (53), transform expression $a_T^2 < a_0^2$ into

$$n^2 - 12 < \frac{4\lambda}{1 - \rho_{00}^2} - 1 - \sqrt{1 + \frac{8\lambda}{1 - \rho_{00}^2}}$$

Then put $u = \frac{4\lambda}{1 - \rho_{00}^2}$ to obtain

$$\sqrt{1 + 2u} < u + 11 - n^2$$

and then, assuming from now on that $u + 11 - n^2 > 0$, obtain

$$u^2 + 2(10 - n^2)u + (10 - n^2)(12 - n^2) > 0 \quad (22)$$

Deduce that u must be outside the interval between the roots, and also greater than $n^2 - 11$, which finally yields:

$$\frac{4\lambda}{1 - \rho_{00}^2} > n^2 - 10 + \sqrt{2(n^2 - 10)} \quad (23)$$

The condition $a_0 < a_T$ yields an inequality opposed to (23).

3.2 Graphical representation of the argumental phenomenon's possibility of existence.

In Section 3.1, it has been shown that the condition of intersection of the β -curve and the G -curve depends only on parameters λ , ρ_{00} , β and n . This condition is the condition of possibility of existence of the argumental phenomenon. Considering that β and f_{00} are fixed for a given configuration of the BUT, and that n is an arbitrary even integer greater or equal to 4 accounting for the gross frequency ratio between the excitation frequency and f_{00} , one is leaded to use the (λ, ρ_{00}) -plane to represent the regions where the argumental phenomenon is possible. Knowing that $\rho_{00} = f_{excit}/(n f_{00})$, the variability of f_{excit} is accounted for by the variability of ρ_{00} , and the variability of F_0 is accounted for

by the variability of λ , with $\lambda = |F_0|/F_B$. Noticing that ρ_{00} appears only as ρ_{00}^2 , preferably use the (λ, ρ_{00}^2) -plane for the graphical representations. By so doing, all parabolas having the axis of abscissae as principal axis become rectilinear lines, so that plots are easier to read and manipulate.

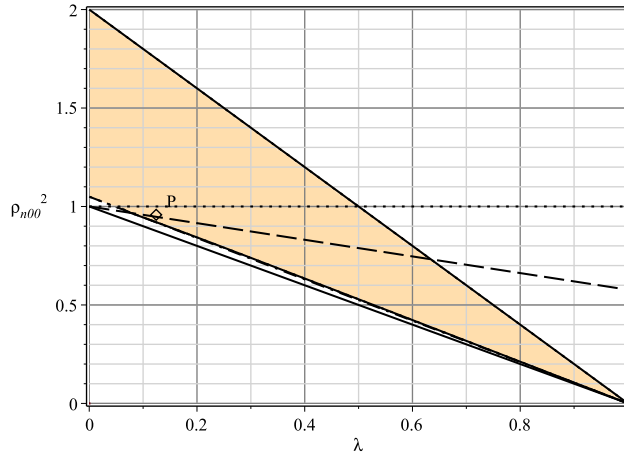


Figure 6: Possibility of existence of the argumental phenomenon (in the shaded region). Parameter values for n , β , F_B , f_{00} and f_{shaker} are the same as for Fig. 16, whose values of λ and ρ_{00} are represented here by point P. The solid lines are the upper and lower limits of the smooth model's validity region. The dotted line is the border between the case $\rho_{00} < 1$ and the case $\rho_{00} > 1$. The dashed line is the border between the case $a_T < a_0$ and the case $a_T > a_0$. The dash-dotted line is the border below which the β -curve and the G -curve don't intersect in the region above the dashed line. The dash-dotted line is not relevant in the region below the dashed line. The solid curve is the curve below which the β -curve and the G -curve don't intersect in the region below the dashed line. It is not relevant above the dashed line.

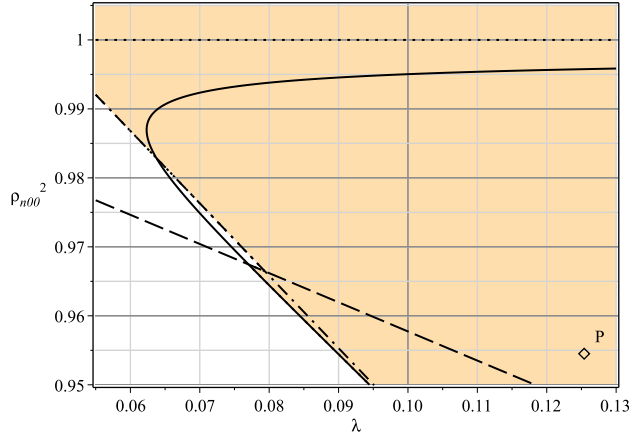


Figure 7: Zoomed view of Fig. 6. The slight offset of the shaded area at $(0.08, 0.967)$ is due to the use of approximated symbolic formulas for a_T and a_0 .

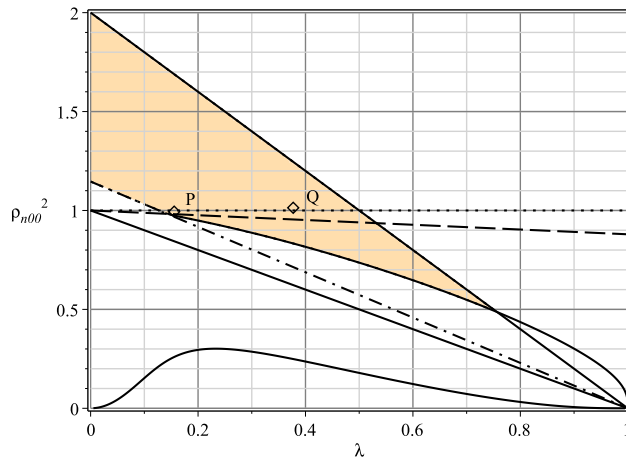


Figure 8: Possibility of existence of the argumental phenomenon (in the shaded region). Parameter values for n , β , F_B and f_{00} are the same as in Figs. 2 and 3. Point P (resp. Q) represents the values of λ and ρ_{00} in Fig. 2 (resp. Fig. 3). The description of the graphic elements is the same as for Fig. 6.

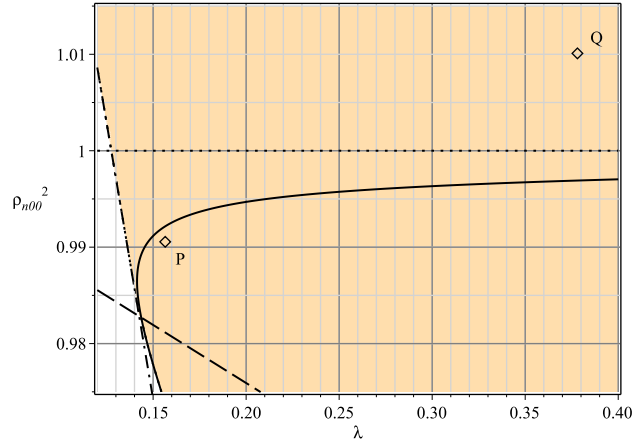


Figure 9: Zoomed view of Fig. 8. The slight offset of the shaded area at $(0.145, 0.983)$ is due to the use of approximated symbolic formulas for a_T and a_0 .

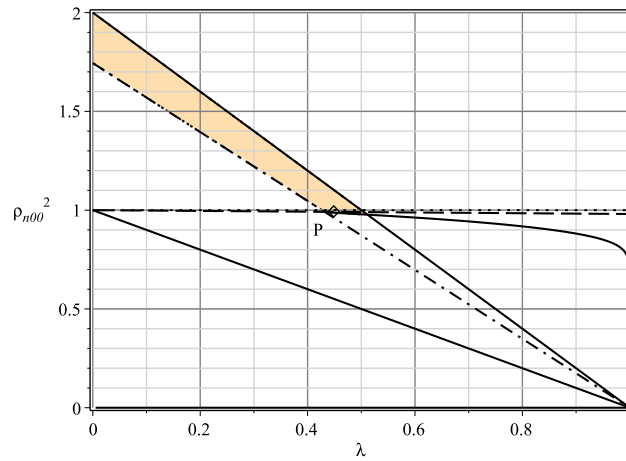


Figure 10: Possibility of existence of the argumental phenomenon (in the shaded region). Parameter values are: $n = 14$, $\beta = 1.6 \cdot 10^{-3}$, $F_B = 51N$, $f_{00} = 6.615Hz$ and $f_{shaker} = 92.1495Hz$, $\rho_{00} = 0.995$, $\lambda = 0.45$. Point P represents the values of λ and ρ_{00} . The description of the graphic elements is the same as for Fig. 6.

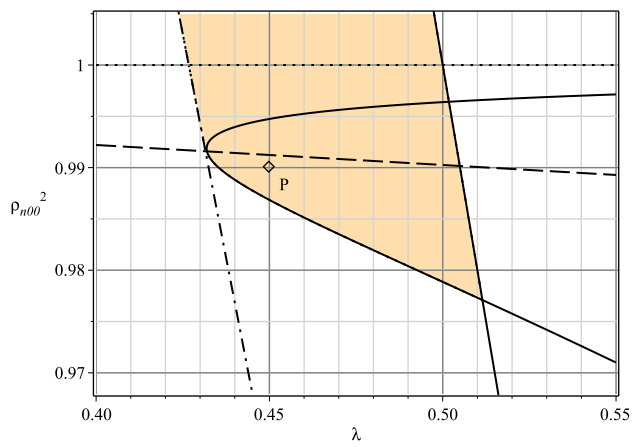


Figure 11: Zoomed view of Fig. 10.

3.3 Validity of the localization of the minimum of the stationary-solutions curve as the intersection of the β -curve and the G -curve.

One purpose of the study of the stationary-solutions curve is to assess the excitation threshold introduced in Section 3, which is the minimum value of the excitation a_A necessary to obtain an argumental phenomenon. So far, the minimum of the stationary-solutions curve, located at point A_{min} in Fig. 2, has been considered close to the intersection of the β -curve and the G -curve. In this section, the validity of this approximation is studied, and an upper bound of the error involved in this approximation is given in symbolic form. An all-case numeric upper bound is then derived. Only the case $\rho_{00} < 1$ is considered, because when $\rho_{00} > 1$, the minimum of the stationary-solutions curve is always above a_{crit} , and it is approached for large values of a_S . In this case, a_{crit} is a convenient lower bound of the stationary-solutions curve.

In the case $\rho_{00} < 1$, said lower bound can get close to 0, and a more detailed study deserves to be carried out.

Parameterized β -curves. Recall the first equation of System (8):

$$\frac{A(a_A)}{4\rho} S_n(a_S) \sin(n\varphi_S) - \beta a_S = 0 \quad (24)$$

with $A(a_A) = \frac{kLa_A}{F_B + F_0}$ as per Equ. (1), knowing that $\rho_{00} < 1$. This equation defines a family of β -curves, parameterized by φ_S . Consider Equ. (24) as defining a function $A(a_S)$ with φ_S as a parameter, and study the way the representative curve evolves in the (a_S, A) -plane when φ_S varies.

From Equ. (3) applied to $a = a_S$, deduce that function $S_n(a_S)$ is always negative and consequently that $\sin(n\varphi_S)$ is negative. Substituting the expression (3) into Equ. (24), obtain

$$A(a_S) = -\frac{\rho\beta}{n \sin(\varphi_S)} \frac{a_S^{n+2} B^{\frac{n}{2}+1}}{\left(\sqrt{1 + Ba_S^2} - 1\right)^n} \quad (25)$$

It follows that when φ_S decreases and comes next to $-\pi/2$, with $-\pi/2 < n\varphi_S < 0$, A decreases. And as A is a monotonic increasing function of a_A , it follows that a_A decreases and that the parameterized β -curves are localized below each other with no contact point between each other, and globally move toward the abscissae axis as φ_S decreases toward $-\pi/2$.

In the (a_S, a_A) -plane, the abscissa of the intersection point of the β -curve and the G -curve has been denoted a_0 . Denote by A_0 the corresponding value of A on the β -curve. Equ. (24) applied at $a_S = a_0$ writes, knowing that $\sin(n\varphi_S) = -1$ at this point:

$$\frac{A_0}{4\rho} S_n(a_0) + \beta a_0 = 0 \quad (26)$$

Develop Equ. (24) to the first order with respect to a_S and to the second order w.r.t. φ to obtain, using Equ. (26):

$$A - A_0 + \left(A_0 \frac{S'_0}{S_0} + \frac{4\rho\beta}{S_0} \right) (a_S - a_0) - A_0 \frac{\epsilon^2}{2} \approx 0$$

with $\epsilon = n\varphi - n\varphi_0$ and $S'_0 = \frac{dS_n}{da}(a_0)$. Using Equ. (26) once again, obtain:

$$\frac{A - A_0}{A_0} + \left(\frac{S'_0}{S_0} - \frac{1}{a_0} \right) (a - a_0) - \frac{\epsilon^2}{2} \approx 0 \quad (27)$$

Parameterized G -curves. Recall the second equation of System (8):

$$G_1(a_S) + \frac{A}{4a_S} D_n(a_S) \cos(n\varphi_S) - \frac{\rho^2 - 1}{2} = 0 \quad (28)$$

This equation defines a family of G -curves, also parameterized by φ_S . Consider Equ. (28) as defining a function $A(a_S)$ with φ_S as a parameter, and study the way the representative curve evolves in the (a_S, A) -plane when φ_S varies.

First notice that this curve family has a fixed point Q located at $(a_0, 0)$, because at this point, $G_1(a_0) - \frac{\rho^2 - 1}{2} = 0$, which is the definition of the G -curve as per Equ. (10), and $A = 0$: it follows that at point Q , Equ (28) holds for all values of φ_S .

Second, substitute $G(a_S)/a_S$ for $G_1(a_S)$ in Equ. (28) and develop to the first order w.r.t. a_S and φ . Because, by definition of A_0 and a_0 , Equ. (28) holds for $a_S = a_0$ and $A = A_0$, with $\cos(n\varphi_0) = 0$ and $\sin(n\varphi_0) = -1$, it holds

$$G(A_0, a_0) - \frac{\rho^2 - 1}{2} a_0 = 0 \quad (29)$$

and consequently, the limited development of Equ. (28) writes:

$$(A - A_0)H_0 + (a_S - a_0)J_0 + \frac{A_0 D_0}{4} \epsilon = 0 \quad (30)$$

with $H_0 = G'_A(A_0, a_0)$, $J_0 = G'_a(A_0, a_0) - (\rho^2 - 1)/2$ and $D_0 = D_n(a_0)$.

Because $\rho_{00} < 1$ and the study is in the region $a_A < a_{Acrit}$, the expression for G is, as per Equ. (6):

$$G(A, a_S) = -\frac{1}{2} \frac{F_0}{F_B + F_0} a \left(1 - \frac{2}{Ca_S^2} + \frac{1}{Ca_S^2} \frac{2}{\sqrt{Ca_S^2 + 1}} \right) \quad (31)$$

It follows that $G'_A(A_0, a_0) = 0$, and consequently, Equ. (30) writes:

$$(a_S - a_0)J_0 + \frac{A_0 D_0}{4} \epsilon = 0 \quad (32)$$

Note that J_0 can be symbolically expressed as

$$J_0 = -\frac{F_0}{F_B + F_0} \frac{1}{Ca_0^2} \left(2 - \frac{3Ca_0^2 + 2}{(Ca_0^2 + 1)^{3/2}} \right) \quad (33)$$

Approached stationary-solutions curve about (A_0, a_0) . To build an approached expression of the stationary-solutions curve about point (A_0, a_0) , eliminate ϵ between the approached expressions (27) and (32) of the parameterized β -curves and G -curves about said point. After a few calculus, obtain:

$$\frac{A_0^2 D_0^2}{8} \frac{A - A_0}{A_0} + \frac{A_0^2 D_0^2}{8} \left(\frac{S'_0}{S_0} a_0 - 1 \right) \frac{a_S - a_0}{a_0} = J_0^2 (a_S - a_0)^2 \quad (34)$$

Consider this as a definition of function A of variable a_S . The representative curve is a parabola. Search an extremum of A by differentiating (34) and writing that $dA/da_S = 0$, thus obtaining

$$\frac{A_m - A_0}{A_0} = - \left(\frac{A_0 D_0}{4 J_0 a_0} \left(\frac{S'_0}{S_0} a_0 - 1 \right) \right)^2 \quad (35)$$

where A_m is the minimum value of A on the approached stationary-solutions curve.

Using Eqs. (4), (5), (26) and (33), obtain

$$\frac{A_m - A_0}{A_0} = - \left(\frac{F_B + F_0}{F_0} \frac{\rho \beta}{\frac{1}{C a_0^2} \left(2 - \frac{3 C a_0^2 + 2}{(C a_0^2 + 1)^{3/2}} \sqrt{1 + B a_0^2} \right)} \left(\frac{n}{\sqrt{1 + B a_0^2}} - 2 \right) \right)^2 \quad (36)$$

with a_0 as per Equ. (21).

Because $\rho_{00} < 1$, Equ. (1) applies, giving $A = \frac{k L a_A}{F_B + F_0}$. It follows that

$$\frac{a_{Am} - a_{A0}}{a_{A0}} = \frac{A - A_0}{A_0} \quad (37)$$

where a_{Am} is the minimum value of a_A on the approached stationary-solutions curve.

Finally, put $\lambda = |F_0|/F_B$, $x = C a_0^2$, and substitute $\rho_{00} \sqrt{\frac{F_B}{F_B + F_0}}$ for ρ to obtain, with the help of Equ (37):

$$\frac{a_{Am} - a_{A0}}{a_{A0}} = - \frac{1 - \lambda}{\lambda^2} \rho_{00}^2 \beta^2 \left(\frac{x}{\left(2 - \frac{3x+2}{(x+1)^{3/2}} \sqrt{1+x/2} \right)} \left(\frac{n}{\sqrt{1+x/2}} - 2 \right) \right)^2 \quad (38)$$

a_{Am} is the approached minimum of the stationary-solutions curve using limited developments of the parameterized β -curve and G -curve, while a_{A0} is the value of a_A at the intersection of the β -curve and the G -curve at abscissa a_0 . Assuming that a_{Am} is the exact value of the stationary-solutions curve's minimum, Equ. (38) gives the relative error on the value of a_{Am} about a_{A0} . Notice that because $\lambda < 1$, this error is always negative, which is in good agreement with the intuition.

Upper bound of the relative error. In the paragraphs below, an upper bound is searched for the expression given in Equ. (38) in the case where the intersection point is below the critical line. If it can be shown that the relative error actually has a small magnitude, this will give foundation to the initial hypothesis according to which the intersection point of the β -curve and the G -curve is close to the minimum of the stationary-solutions curve and, consequently, to the procedure of limited development applied to the β -curve, the G -curve and the stationary-solutions curve.

In the (λ, ρ_{00}^2) -plane, define:

- A “grey zone” as the region where an intersection exists between the β -curve and the G -curve under the critical line in the (a_S, a_A) -plane.
- An “orange zone” as the region where the relative error on a_{Am} , i.e. $\frac{a_{Am} - a_{A0}}{a_{A0}}$, is below a given threshold.

Each of these zones has a shape which depends on the system’s parameters and the error threshold. It will be shown in the paragraphs below that the grey zone is entirely included in an orange zone corresponding to an appropriate threshold. Then it will be shown that there is a global maximum for all the possible thresholds involved in this process, and that this global minimum is independent of any system parameter. This will show that the relative error on a_{Am} admits a small upper bound independent of the system parameters.

The grey zone. Note that Equ. (20) is also valid for $a_0 > a_T$, but, when in this case, is more restrictive than Equ. (17), because it is limited to the region below the critical line. However, it will be of use here, because the condition of intersection below the critical line is now to be studied regardless of the respective values of a_T and a_0 . By definition, Equ. (20) defines the grey zone in the (λ, ρ_{00}^2) -plane. Rearrange this equation by putting $z = Ba_0^2$:

$$\rho_{00}\beta \frac{\sqrt{1-\lambda}}{\lambda} < \frac{1}{z} \left(\frac{\sqrt{1+z}-1}{\sqrt{z}} \right)^n \quad (39)$$

The developed expression for z is given in Equ. (21) as:

$$z = \frac{\lambda}{1-\rho_{00}^2} - \frac{1}{4} - \frac{1}{4} \sqrt{1 + 8 \frac{\lambda}{1-\rho_{00}^2}} \quad (40)$$

The orange zone. Equ. (38) gives the definition of the relative error on a_{Am} , and thus, knowing that expression (38) is always negative, the orange zone can be defined by:

$$\frac{1-\lambda}{\lambda^2} \rho_{00}^2 \beta^2 \left(\frac{2z}{2 - \frac{6z+2}{(2z+1)^{3/2}} \sqrt{1+z}} \left(\frac{n}{\sqrt{1+z}} - 2 \right) \right)^2 < ErrMax \quad (41)$$

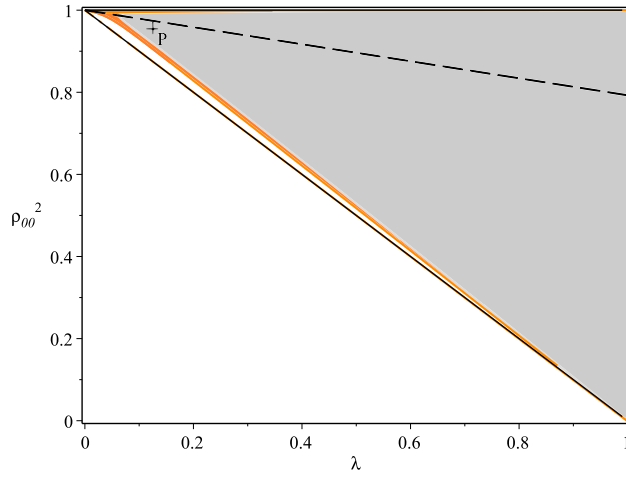


Figure 12: Grey zone and orange zone. Parameters: same as Fig. 16. Point P represents the ρ_{00} and λ values of Fig. 16. The orange zone is drawn for $ErrMax = 0.008$.

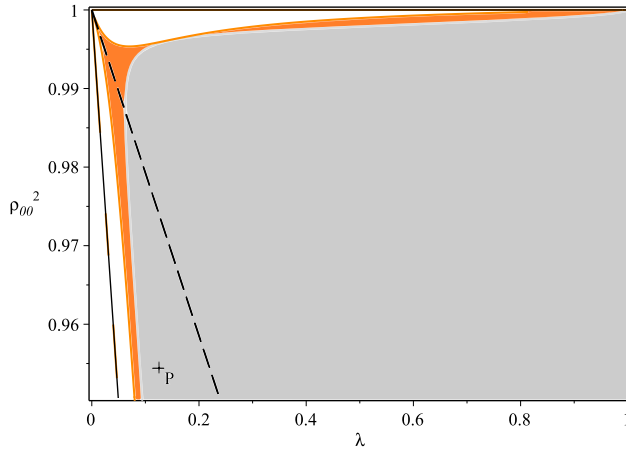


Figure 13: Zoomed view of Fig. 12.

where $ErrMax$ is a given value of the maximum acceptable relative error inside the orange zone, and $z = Ba_0^2 = x/2$.

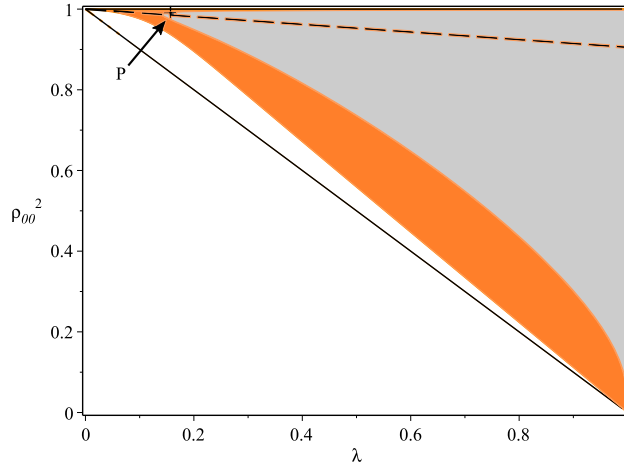


Figure 14: Grey zone and orange zone. Parameters: same as Fig. 2. Point P represents the ρ_{00} and λ values of Fig. 2. The orange zone is drawn for $ErrMax = 0.0195$.

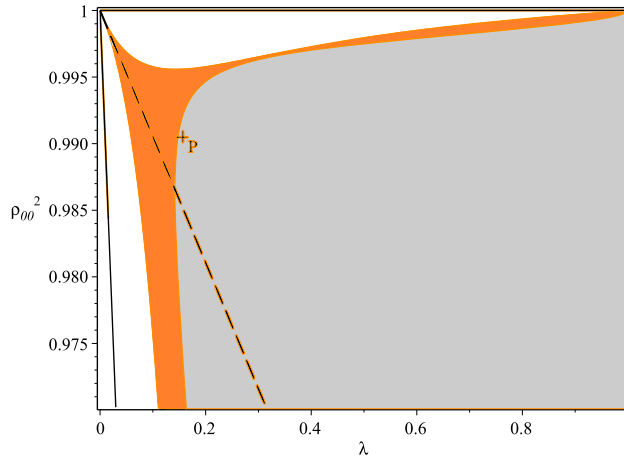


Figure 15: Zoomed view of Fig. 14.

Points in the orange zone where the relative error vanishes. Notice that when $\lambda \neq 0$ and

$$\frac{n}{\sqrt{1+z}} - 2 = 0 \quad (42)$$

inequality (41) is always defined and is verified for $ErrMax = 0$. Substituting expression (40) for z in (42), and rearranging, yields

$$\rho_{00}^2 = 1 - \lambda/k_1 \quad (43)$$

with $k_1 = n^2/2 - 1 + 1/2\sqrt{n^2/2 - 1}$.

This is a straight line in the (λ, ρ_{00}^2) -plane, passing through point $(\lambda = 0, \rho_{00}^2 = 1)$. This line is included in the orange zone, in the region $0 < \lambda < 1$.

A point in the orange zone which is not included in the grey zone.

Along this line, Equ. (42) holds, which means that $z = n^2/4 - 1$. Substituting this expression for z in Equ. (39) yields the condition for points on said line to be included in the grey zone:

$$\rho_{00}\beta\frac{\sqrt{1-\lambda}}{\lambda} < N \quad (44)$$

with $N = \frac{1}{n^2/4 - 1} \left(\frac{n/2 - 1}{\sqrt{n^2/4 - 1}} \right)^n$ being a constant.

In (44), substituting ρ_{00} for its expression (43) yields

$$\sqrt{1 - \frac{\lambda}{k_1}} \beta \frac{\sqrt{1-\lambda}}{\lambda} < N \quad (45)$$

And because the limit of the left-hand member is $+\infty$ when λ approaches 0, there is a value λ_0 below which the points on the line are not inside the grey zone. It follows that, on the line defined by (43), point at abscissa $\lambda_0/2$ is in the orange zone but not in the grey zone.

A point included in both the orange zone and the grey zone. One point which is inside both zones is $(\lambda = 1, \rho_{00}^2 = 7/15)$. At this point, $z = 5/8$, and inequalities (39) and (41) are verified.

Contact condition between the borders of the grey zone and the orange zone. For a given grey zone, if it can be shown that for a sufficiently large value of *ErrMax*, there is no contact point between said borders, it will be possible to conclude that the grey zone is entirely contained inside the orange zone, because it has been shown above that their interiors have at least one point in common and that the orange zone contains at least one point which is not inside the grey zone. Then it will be possible to conclude that the relative error inside the whole grey zone, i.e. for all intersection points of the β -curve and the G -curve below the critical line, is below *ErrMax*.

Intersection of the borders of the grey zone and the orange zone.

Equ. (41) can be written

$$\sqrt{\frac{1-\lambda}{\lambda^2}} \rho_{00}\beta \left| \frac{2z}{2 - \frac{6z+2}{(2z+1)^{3/2}} \sqrt{1+z}} \left(\frac{n}{\sqrt{1+z}} - 2 \right) \right| < \sqrt{ErrMax} \quad (46)$$

Eliminate $\rho_{00}\beta\frac{\sqrt{1-\lambda}}{\lambda}$ between the border equations corresponding to inequalities (39) and (46) to obtain the equation of the intersection of the borders of the grey zone and the orange zone:

$$\sqrt{ErrMax} = \frac{2 \left| \frac{n}{\sqrt{1+z}} - 2 \right| \left(\frac{\sqrt{z+1}-1}{\sqrt{z}} \right)^n}{\left| 2 - \frac{6z+2}{(2z+1)^{3/2}} \right| \sqrt{1+z}} \quad (47)$$

A numerical study of the function of z at the right-hand member of this equation for $0 \leq z \leq 1000$ and $4 \leq n \leq 1000$ shows that its magnitude is always less than 0.14. It follows that if the magnitude of $ErrMax$ is greater than $0.14^2 \approx 2 \cdot 10^{-2}$, Equ. (47) has no solution, and consequently, that the grey zone is entirely included in the orange zone, because there exists at least one point inside the orange zone which is not inside the grey zone, and there exists at least one point inside both zones.

Conclusion about the relative error. The result above means that, over large ranges of z and n , when the β -curve and the G -curve intersect below the critical line in the (a_S, a_A) -plane, the relative error caused by the substitution of the ordinate a_{A0} of the intersection of the β -curve and the G -curve for the minimum a_{Am} of the stationary-solutions curve is lower than $2 \cdot 10^{-2}$.

3.4 Approximate symbolic solution for the intersection above the critical line.

In this section, the intersection of the β -curve and the G -curve is assessed when above the critical line. As for the intersection below the critical line, it arises at an abscissa a_0 which is calculated in Appendix B. Then, substituting a_0 for a_S in the lower β -curve's equation (18) yields the ordinate of the intersection point. If the conditions of intersection studied above are satisfied, it is possible to solve approximately Eq. (48) by putting $z = Ba_S^2$ and using the following remarks:

- Function $1 - \frac{1}{z} + \frac{1}{z\sqrt{2z+1}}$ can be approximated by function $\frac{\sqrt{2}z}{1 + \sqrt{2}z}$.
- Function $J(z) = \frac{1}{z} \left(\frac{\sqrt{1+z}-1}{\sqrt{z}} \right)^n$ can be approximated by function

$$K(z) = \frac{hz}{bz^2 + cz + 1},$$

$$\text{with } c = 8 \frac{n^2 + 4}{(n^2 - 4)^2}, b = \frac{16}{(n^2 - 4)^2}, \text{ and } h = \frac{4}{n^2 - 4} \left(\frac{n-2}{n+2} \right)^{n/2} \left(c + \frac{8}{n^2 - 4} \right) = \frac{64n^2}{(n^2 - 4)^3} \left(\frac{n-2}{n+2} \right)^{n/2}.$$

Thus, Eq. (48) becomes:

$$E \frac{\sqrt{2}z}{1 + \sqrt{2}z} = \frac{hz}{bz^2 + cz + 1}$$

with $E = \frac{\rho\beta}{\rho^2 - 1}$. This is a second-degree equation in z , which, once solved in z , and due to the definition of z by $z = Ba_S^2$, yields the abscissae of points A_{min-} and A_{min+} . This second-degree equation in z is:

$$E\sqrt{2}bz^2 + \sqrt{2}(Ec - h)z + E\sqrt{2} - h = 0$$

The condition to have real roots is: $2(Ec - h)^2 - 4E\sqrt{2}(E\sqrt{2} - h) \geq 0$. Then, using Eq. (48), the ordinates of said points can be calculated. Those points are represented in Fig. 2.

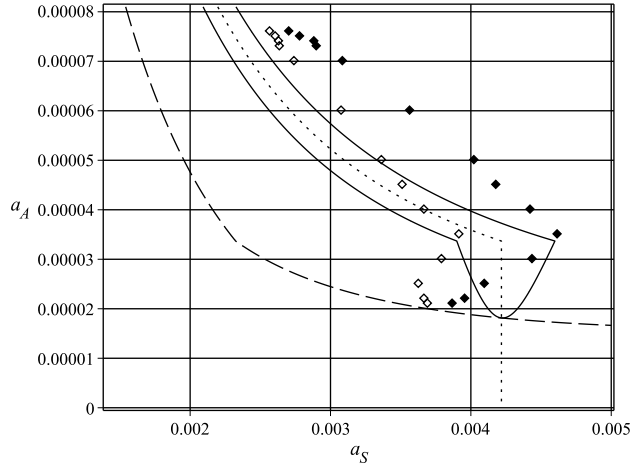


Figure 16: Stationary condition, a_A (point A's amplitude) against a_S (stationary motion's amplitude). Comparison between second-order equation (with natural model), represented as diamonds, and averaged system (with smooth model), represented as a solid line. The G -curve is the dotted line, while the β -curve is the dashed line. Parameters are: $n = 4$, $F_B = 51N$, $F_0 = -6.4N$, $f_{00} = 6.615Hz$, $\beta = 2.4 \cdot 10^{-3}$, $L = 0.95m$, $k = 200 \cdot 10^{-3}N/m$, $\nu = 162.419s^{-1}$, $\rho_{00} = 0.976938$, $\lambda = 0.1254$. In the same way as in Fig. 2, where stable and unstable stationary solutions are represented as an infinity of points belonging to solid lines, a discrete series of stable (solid diamonds) and unstable (diamonds) stationary points are represented here. Model validity upper limit= $2.347 \cdot 10^{-4}$.

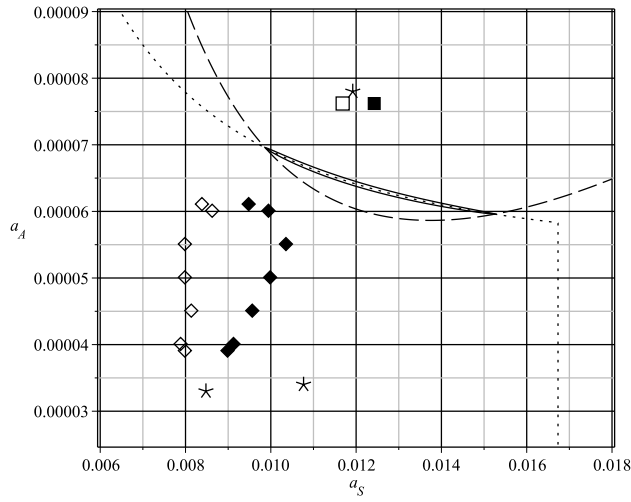


Figure 17: Stationary condition, a_A (point A's amplitude) against a_S (stationary motion's amplitude). Comparison between second-order equation (with natural model) and averaged system (with smooth model). Parameters are the same as in Fig. 2, except $F_0 = -7.2N$. In the same way as in Fig. 2, stable and unstable stationary points are represented. Results of numerical simulations using the natural model are represented as diamonds (unstable points) and solid diamonds (stable points). Model validity upper limit= $3.54 \cdot 10^{-4}$.

4 Conclusion.

It has been presented a symbolic study of the stationary transverse vibrations of a system consisting of a beam submitted, through a permanent or an intermittent elastic contact, to an harmonic axial excitation which is an even multiple (greater than 2) of the beam's fundamental transverse frequency. This constitutes an argumental phenomenon.

An symbolic approximation giving a symbolic expression of the excitation threshold as a function of the physical system's parameters has been given, as the intersection of two curves in the (oscillator's amplitude, excitation's amplitude)-plane, whose symbolic expressions have been brought out.

A study of the validity of said approximation has yielded a symbolic expression of the relative error and confirmed that this error is in all cases lower than 2%.

A study of the symbolic limit conditions for the argumental phenomenon to arise has been given and represented in the (λ, ρ_{00}^2) -plane.

A study of the symbolic limit conditions for permanent contact seems of interest. Numerical simulations show that this case may arise under ordinary conditions.

5 Appendix A: tangency condition between the upper β -curve and the upper G -curve.

In this Appendix, the tangency condition between the curves representing the upper G -function

$$a_{A1}(a) = \frac{F_0}{kL} + 2 \frac{F_B}{kL} \frac{(\rho^2 - 1)Ca^2}{\rho^2 Ca^2 - 2 + \frac{2}{\sqrt{Ca^2+1}}}$$

and the upper beta-function

$$a_{A2}(a) = \frac{F_0}{kL} + 2 \frac{F_B}{kL} \frac{1}{1 + \frac{1}{\rho\beta} \frac{1}{Ba^2} \left(\frac{\sqrt{1+Ba^2}-1}{\sqrt{Ba^2}} \right)^n}$$

will be studied in the (a, a_A) -plane for a real positive and n integer with $n \geq 4$. The equation of the intersection between $a_{A1}(a)$ and $a_{A2}(a)$ will first be formed, then the tangency condition will be studied.

Equation of the intersection between $a_{A1}(a)$ and $a_{A2}(a)$. Write $a_{A1}(a) = a_{A2}(a)$ and substitute the developed expressions of $a_{A1}(a)$ and $a_{A2}(a)$ given above, then carry out basic calculus to obtain, denoting Ba^2 by z for clarity:

$$\frac{1}{z} \left(\frac{\sqrt{1+z}-1}{\sqrt{z}} \right)^n = E \left(1 - \frac{1}{z} + \frac{1}{z\sqrt{1+2z}} \right) \quad (48)$$

with $E = \frac{\rho\beta}{\rho^2 - 1}$. The tangency condition between the curves of $a_{A1}(a)$ and $a_{A2}(a)$ for $a > 0$ is the same as the tangency condition between the functions $y_1(z) = E \left(1 - \frac{1}{z} + \frac{1}{z\sqrt{1+2z}} \right)$ and $y_2(z) = \frac{1}{z} \left(\frac{\sqrt{1+z}-1}{\sqrt{z}} \right)^n$ for $z > 0$. What is searched is a condition on E .

So the curves representing function $y_1(z) = E \left(1 - \frac{1}{z} + \frac{1}{z\sqrt{2z+1}} \right)$ and function $y_2(z) = \frac{1}{z} \left(\frac{\sqrt{1+z}-1}{\sqrt{z}} \right)^n$ will be studied for z real positive, $n \geq 4$, and $E =$ positive constant.

Function $y_1(z) = E \left(1 - \frac{1}{z} + \frac{1}{z\sqrt{2z+1}} \right)$. This function is an increasing function for $z > 0$. Near zero, the function is equivalent to $3z/2 - 5z^2/2$. The asymptotic limit for $z \rightarrow +\infty$ is 1. The plot for $E = 1$ is given in Fig. 18.

Function $y_2(z) = \frac{1}{z} \left(\frac{\sqrt{1+z}-1}{\sqrt{z}} \right)^n$. This function is defined for every real positive z , and can be extended to 0 in $z = 0$.

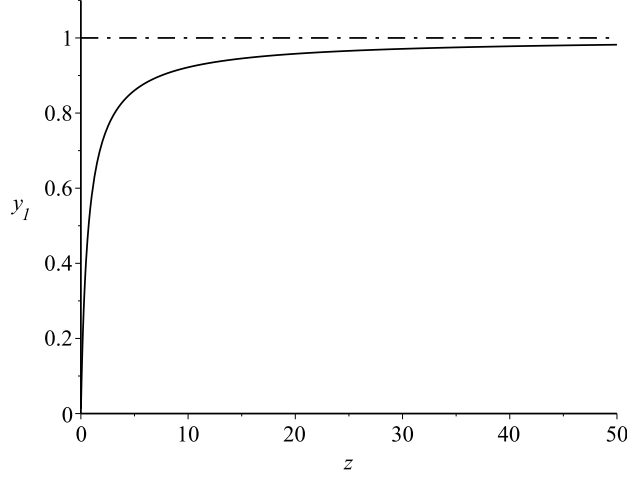


Figure 18: Plot of $y_1(z)$, with $E = 1$.

Near zero, the function is equivalent to $\frac{z^{\frac{n}{2}-1}}{2^n}$.

Near infinity, the function is equivalent to $\frac{1}{x} \left(1 - \frac{n}{\sqrt{z}}\right)$.

The function increases from $z = 0$ to $z_{2max} = \frac{n^2}{4} - 1$, then decreases asymptotically to 0.

The value of the maximum is $y_{2max} = \frac{4}{n^2 - 4} \left(\frac{n-2}{n+2}\right)^{n/2}$.

The plot for $n = 6$ is given in Fig. 19.

Tangency of functions $y_1(z)$ and $y_2(z)$. Knowing the behaviour of functions y_1 and y_2 , one is led to consider that when those curves are tangent, the tangency point is approximately at the maximum of y_2 , provided that $y_1(z_{2max}) = y_{2max}$. Hence the value E_T of E which satisfies this tangency must verify:

$$E_T \left(1 - \frac{1}{z_{2max}} + \frac{1}{z_{2max} \sqrt{2z_{2max} + 1}}\right) = \frac{4}{n^2 - 4} \left(\frac{n-2}{n+2}\right)^{n/2}$$

Using the approximation

$$1 - \frac{1}{z_{2max}} + \frac{1}{z_{2max} \sqrt{2z_{2max} + 1}} \approx 1 - \frac{4}{n^2} \quad (49)$$

for $n \geq 4$, finally obtain:

$$E_T \approx \frac{4n^2}{(n^2 - 4)^2} \left(\frac{n-2}{n+2}\right)^{n/2} \quad (50)$$

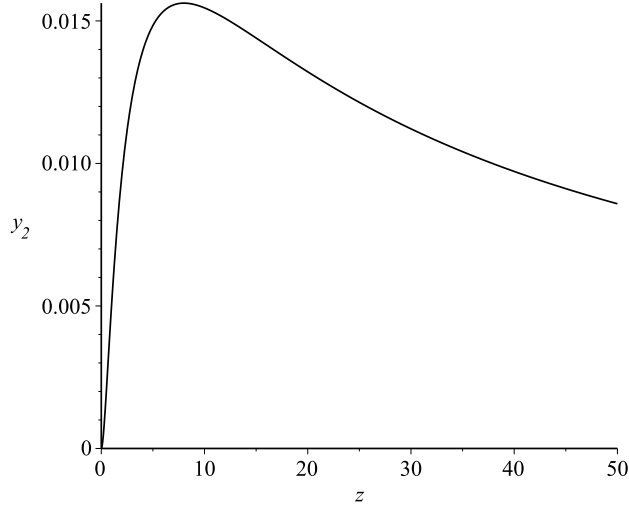


Figure 19: Plot of $y_2(z)$, with $n = 6$.

with $E_T = \frac{\rho\beta}{\rho^2 - 1}$. As for the tangency point's ordinate, assume that it is the same as the maximum of the $y_2(z)$ curve, i.e. y_{2max} . Note that $E_T = \frac{n^2}{n^2 - 4} y_{2max}$.

The following hypothesis are made:

- For $E < E_T$, the curves of y_1 and y_2 intersect at $z = 0$ and at least at two other points, one located at $z < z_{2max}$ and one at $z > z_{2max}$.
- For $E > E_T$, the curves of y_1 and y_2 intersect at $z = 0$.

A typical case is represented in Fig. 20 for $n = 6$ and $E_T = 9/512$ according to Eq. (50). On the plots, it can be seen that the value of y_1 in z_{2max} is slightly greater than expected. This is due to approximation (49), which partially compensates for a better tangency estimate. Other values of n give similarly good results for E_T , except for $n = 4$, where it is better to use a value of $1.03 E_T$.

Basis for a numerical study. To assess the relative error on z_T , form an equation giving the exact value of the tangency abscissa, by putting $y(z) = y_1(z) - y_2(z)$ and writing that both $y(z) = 0$ and $dy/dz = 0$. First transform the equation $y(z) = 0$ to obtain

$$E \left(z - 1 + \frac{1}{\sqrt{1 + 2z}} \right) = \left(\frac{\sqrt{1 + z} - 1}{\sqrt{z}} \right)^n \quad (51)$$

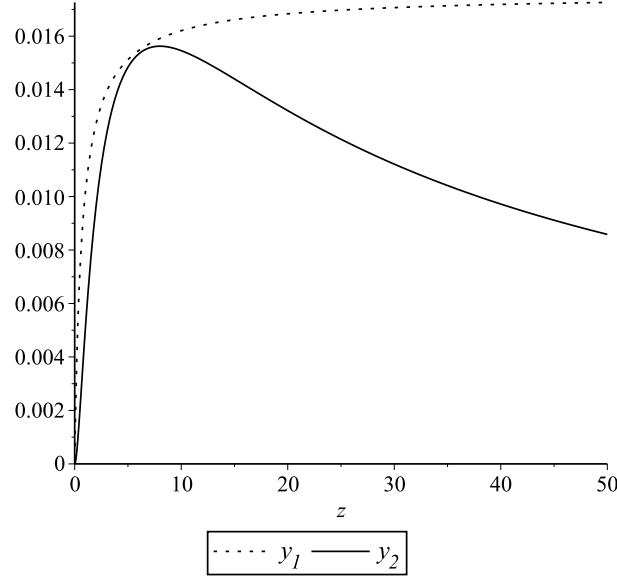


Figure 20: Tangency of $y_1(z)$ and $y_2(z)$, with $n = 6$.

Then calculate $dy/dz(z)$ to obtain

$$\frac{dy}{dz} = \frac{E}{z^2} \left(1 - \frac{1}{\sqrt{2z+1}} - \frac{z}{(2z+1)^{3/2}} \right) + \frac{1}{z^2} \left(\frac{\sqrt{1+z}-1}{\sqrt{z}} \right)^n \left(1 - \frac{n}{2\sqrt{1+z}} \right)$$

and put $dy/dz(z) = 0$. Then write $y(z) = \frac{dy}{dz}(z)$ and, based on Eq. (51), substitute $E \left(z - 1 + \frac{1}{\sqrt{1+2z}} \right)$ for $\left(\frac{\sqrt{1+z}-1}{\sqrt{z}} \right)^n$ to obtain:

$$\sqrt{2z+1} - 1 - \frac{z}{2z+1} = ((z-1)\sqrt{2z+1} + 1) \left(\frac{n}{2\sqrt{1+z}} - 1 \right) \quad (52)$$

On the basis of the study above, which concludes that z_{2max} is a good approximation for the abscissa of the tangency point, try the expression $z_T = \frac{n^2}{4} - 1$ to assess an approximate solution to Eq. (52). A numerical analysis, based on the numerical solutions in z of Eq. (52), shows that this results in a good approximation for z_T , except for the lower values of n . It also shows that if the expression for z_T is changed to become

$$z_T = \frac{n^2}{4} - 3 \quad (53)$$

the approximation is much better for the lower values of n , without being noticeably modified for the higher values. Note that the asymptotic development

(49), which is limited to second-order in $1/n$, is unchanged by this adjustment; the modification shows up only at the fourth-order term. Consequently, the formula giving E is also unchanged. The formula $z_T = \frac{n^2}{4} - 3$ yields a maximum relative error of +3.25% on E at $n = 4$, and -0.8% at $n = 6$. For the other values of n beyond 6, the relative error is negative and has a magnitude below 0.8%. As a conclusion, the chosen formulas for z_T and E_T are those given in Eqs. (50) and (53).

6 Appendix B: position of the G -curve versus the critical line.

In this Appendix, the position of the G -curve versus the critical line is studied, and a simple condition on ρ_{00} is brought out, indicating whether the G -curve is entirely above the critical line or if it intersects said line.

Eqs. (6) and (7) show that the G -curve has a different equation, depending on whether the region of interest is above or under the critical line. This appears in Figs. 2 and 3. Therefore, to study the intersection between the G -curve and the critical line, first study the behaviour of the G -curve when the G -function is expressed as in Eq. (7), i.e. when the current point on the G -curve is above the critical line. The equation of the G -curve above the critical line is given by Equ. (7):

$$\frac{G(a, a_A)}{a} = \frac{\rho^2 - 1}{2} = -\frac{1}{2} \frac{F_0 - a_A kL}{2F_B + F_0 - a_A kL} \left(1 - \frac{2}{Ca^2} + \frac{1}{Ca^2} \frac{2}{\sqrt{1 + Ca^2}} \right)$$

which yields $a_A = \frac{y(a)}{kL}$, with

$$y(a) = F_0 + 2F_B \frac{(\rho^2 - 1)Ca^2}{\rho^2 Ca^2 - 2 + \frac{2}{\sqrt{Ca^2 + 1}}} \quad (54)$$

Notation In this Appendix, the value $\frac{|F_0|}{F_B}$ will be denoted by λ .

Definition domain. The definition domain of $y(a)$ is:

- If $\rho^2 < 1$: $\mathbb{R}^+ \setminus \{a_2\}$ and $\lim_{a \rightarrow a_2^-} y(a) = +\infty$, $\lim_{a \rightarrow a_2^+} y(a) = -\infty$
- If $\rho^2 > 1$: \mathbb{R}^+

with

$$a_2 = \sqrt{\frac{2}{\rho^2 C} - \frac{1 + \sqrt{1 + \frac{8}{\rho^2}}}{2C}} \quad (55)$$

Limit at 0 and at $+\infty$. It holds $\lim_{a \rightarrow 0^+} y(a) = F_0 + 2F_B$. The function $y(a)$ can be extended by continuity to $2F_B + F_0$ at $a = 0$.

Also:

$$\lim_{a \rightarrow +\infty} y(a) = F_0 + 2F_B \frac{\rho^2 - 1}{\rho^2} = 2 \left(1 - \frac{1}{\rho_{00}^2} \right) (F_B + F_0) - F_0 \quad (56)$$

and therefore:

- If $\rho^2 < 1$, i.e. $\rho_{00}^2 < 1 - \lambda$, this limit is negative.

- If $\rho^2 > 1$, this limit is negative or positive:
 - If $1 - \lambda < \rho_{00}^2 < 1$, this limit is lower than $|F_0|$.
 - If $1 < \rho_{00}^2$, this limit is higher than $|F_0|$.

Direction of variation. The derivative $\frac{dy}{da}$ is the same sign as $1 - \rho^2$. Therefore, if $\rho < 1$, $y(a)$ is increasing.

Intersection with the critical line. Recall that the critical line is $\frac{a_A}{kL} = \frac{|F_0|}{F_B}$, i.e. $y(a) = |F_0| = -F_0$. Substituting this value for $y(a)$ and $\rho_{00}^2 \frac{F_B}{F_B + F_0}$ for ρ^2 in Eq. (54) yields

$$(\rho_{00}^2 - 1)Ca^2 = 2\frac{F_0}{F_B} \left(1 - \frac{1}{\sqrt{Ca^2 + 1}} \right)$$

with $a \neq 0$. Put $x = \sqrt{Ca^2 + 1}$, and rearrange terms to obtain, discarding the case $x = 1$:

$$x^2 + x - 2R = 0 \tag{57}$$

with $R = -\frac{F_0}{F_B(1 - \rho_{00}^2)}$ and therefore, $R > 0$ because $\rho_{00}^2 < 1$ and $F_0 < 0$. Discard the negative root, and write that the positive root is greater than 1 to obtain the condition $R > 1$, i.e. $\rho_{00}^2 > 1 - \frac{|F_0|}{F_B}$.

Finally, the condition for the intersection of the G -curve and the critical line to exist is

$$1 - \lambda < \rho_{00}^2 < 1 \tag{58}$$

with $\lambda = \frac{|F_0|}{F_B}$.

To calculate the abscissa a_0 of said intersection, use relation $x^2 - 1 = Ca^2$ together with Eq. (57) to obtain

$$a_0^2 = \frac{|F_0|}{\pi^2 kL} \left(\frac{4\lambda}{1 - \rho_{00}^2} - 1 - \sqrt{1 + \frac{8\lambda}{1 - \rho_{00}^2}} \right) \tag{59}$$

Allowed values for ρ and ρ_{00} . It has been shown in [5] that a necessary condition for the smooth model to be valid is that $a_A kL < F_B + F_0$. Therefore:

- If $\rho < 1$, i.e. $\rho_{00}^2 < 1 - \lambda$, and because $y(a)$ is then always increasing and $y(0) = 2F_B + F_0 > F_B + F_0$, it can be seen that $y(a)$ will never go under $F_B + F_0$ for $0 \leq a < a_2$ (a_2 as defined in Eq. (55)), so that said model is not valid over this interval; it is not valid either for $a_2 < a$, because in this case, $y(a) < 0$. As a conclusion, this case must be discarded.

- If $\rho > 1$, i.e. $1 - \lambda < \rho_{00}^2$, and because the G -curve starts at $a_A = 2F_B + F_0$ for $a = 0$ and is always decreasing, it then can enter the validity domain of the smooth model if it crosses the horizontal line $a_A = (F_B + F_0)/(kL)$. However, for this to happen, it is necessary that $\lim_{a \rightarrow +\infty} y(a) < F_B + F_0$, i.e., using Eq. (56), $\rho_{00}^2 < 2(1 - \lambda)$. If this condition is met, $y(a)$ then decreases to a finite value lower than $|F_0| = kLa_{Acrit}$. So:
 - If $1 - \lambda < \rho_{00}^2 < 1$, the function $a_A(a)$ intersects the critical line $a_A = a_{Acrit} = |F_0|/(kL)$ at $a_S = a_0$, then decreases toward a limit lower than a_{Acrit} , which means that the function never intersects again the critical line.
 - If $1 < \rho_{00}^2$, the function $a_A(a)$ is entirely located above the critical line.
 - * If $1 < \rho_{00}^2 < 2(1 - \lambda)$, at least a part of the G -curve is in the validity domain of the smooth model. This condition implies $\lambda < 1/2$.
 - * If $2(1 - \lambda) < \rho_{00}^2$, there is no part of the G -curve is in the validity domain of the smooth model. This condition must be discarded.

Conclusion. The approached smooth model can be studied only if

$$1 - \lambda < \rho_{00}^2 < 2(1 - \lambda)$$

- If $1 - \lambda < \rho_{00}^2 < 1$, the G -curve has an upper part above the critical line, then a lower part consisting of a vertical segment.
- If $1 < \rho_{00}^2 < 2(1 - \lambda)$, the G -curve is entirely located above the critical line.

References

- [1] M.J. Béthenod. Sur l'entretien du mouvement d'un pendule au moyen d'un courant alternatif de fréquence élevée par rapport à sa fréquence propre. *Comptes rendus hebdomadaires de l'Académie des sciences*, 207(19):847–849, November 1938. (in French).
- [2] D. Cintra and P. Argoul. Non-linear argumental oscillators: Stability criterion and approximate implicit analytic solution. *Journal to be determined*, 2016. (submitted).
- [3] D. Cintra and P. Argoul. Nonlinear argumental oscillators: A few examples of modulation via spatial position. *Journal of Vibration and Control*, 2016. (online publication, pre-printing).
- [4] D. Cintra and P. Argoul. Attractor's capture probability in nonlinear argumental oscillators. *Communications in Nonlinear Science and Numerical Simulation*, 48:150 – 169, 2017.
- [5] D. Cintra, G. Cumunel, and P. Argoul. Transverse argumental vibration of a beam excited axially by an harmonic motion transmitted through permanent or intermittent elastic contact: modeling and numerical results. *Journal to be determined*, 2017. (submitted).
- [6] D. Cintra, G. Cumunel, and P. Argoul. Transverse vibration of a beam excited axially by an harmonic motion transmitted through intermittent elastic contact: experimental results. *Journal to be determined*, 2017. (submitted).
- [7] B. Cretin and D. Vernier. Quantized amplitudes in a nonlinear resonant electrical circuit. In *2009 Joint Meeting of the European Frequency and Time Forum and the IEEE International Frequency Control Symposium, vols 1 and 2*, volume 1 & 2, pages 797–800, Besançon, France, April 2009. Joint Meeting of the 23rd European Frequency and Time Forum/IEEE International Frequency Control Symposium.
- [8] D. Doubochinski. *Argumental oscillations. Macroscopic quantum effects*. SciTech Library, August 2015.
- [9] D.B. Doubochinski and J.B. Doubochinski. Amorçage argumentaire d'oscillations entretenues avec une série discrète d'amplitudes stables. *E.D.F. Bulletin de la direction des études et recherches, série C mathématiques, informatique*, 3:11–20, 1991. (in French).
- [10] D. I. Penner, D. B. Doubochinski, M. I. Kozakov, A. S. Vermel, and Yu. V. Galkin. Asynchronous excitation of undamped oscillations. *Soviet Physics Uspekhi*, 16(1):158–160, July-August 1973.

- [11] J.P. Treilhou, J. Coutelier, J.J. Thocaven, and C. Jacquez. Payload motions detected by balloon-borne fluxgate-type magnetometers. *Advances in Space Research*, 26(9):1423–1426, 2000.